Ion-exchanged waveguide add/drop filter

David F. Geraghty, Dan Provenzano, Michael M. Morrell, Seppo Honkanen, Amnon Yariv, et al.

David F. Geraghty, Dan Provenzano, Michael M. Morrell, Seppo Honkanen, Amnon Yariv, Nasser Peyghambarian, "Ion-exchanged waveguide add/drop filter," Proc. SPIE 4277, Integrated Optics Devices V, (15 May 2001); doi: 10.1117/12.426828

SPIE.

Event: Symposium on Integrated Optics, 2001, San Jose, CA, United States

Ion-Exchanged Waveguide Add/Drop Filter

D. F. Geraghty[a], D. Provenzano[b], M. M. Morrell[a], S. Honkanen[a], A. Yariv[b], N. Peyghambarian[a,c]

[a] NP Photonics, UA Science and Technology Park, 9030 S. Rita Road, Suite 120, Tucson, AZ 85747
[b] California Institute of Technology, Applied Physics Dept., Mail Code 128-95, Pasadena, CA 91125
[c] University of Arizona, Optical Sciences Center, Tucson, AZ 85721

Abstract

An add/drop filter with a two-moded section is demonstrated using buried ion-exchanged waveguides and a photowritten Bragg grating. The device exhibits a 20 dB extinction ratio and a 3 dB bandwidth of 0.4 nm (100 GHz).

Keywords: ion-exchange, WDM, add/drop filter, Bragg grating

1. Introduction

Add/drop filters provide a critical functionality in all-optical WDM networks. Extensive work has been done in the area using a variety of optical materials. Ion-exchanged waveguides are a commercially viable medium for integrated optics. They have demonstrated low propagation loss[1], negligible birefringence[2] and photosensitivity[3]. Numerous devices have been fabricated using this technology[1]. In this article we report the demonstration of an add/drop filter using buried ion-exchanged waveguides and photowritten Bragg gratings.

2. Device Principles

2.1 Device Operation

The device design is similar to fiber[4] and silica-on-silicon[5] waveguide technology devices previously reported. A schematic is shown in Figure 1. Two single mode waveguides of different widths are brought together adiabatically into a two-mode section. The two-mode section is again later separated into the two single mode waveguides. Bragg gratings are written at a small angle in the two-mode section. The filter functions as follows. Input signals on the narrow waveguide are coupled to the odd mode of the two-mode section. For wavelengths on resonance, a tilted grating breaks the orthogonality of the two modes and reflects the signal to the backwards propagating even mode. This propagates back out the wide "drop" port. Wavelengths off resonance pass through the Bragg grating and continue on to the narrow output port. Additionally, a signal on resonance at the dropped wavelength can be added through the fourth port.

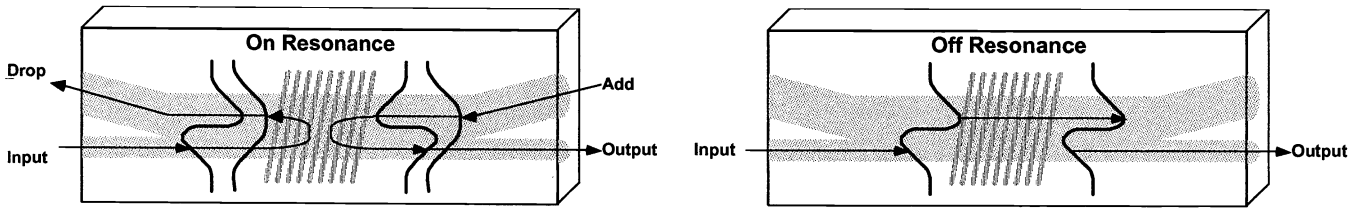

Figure 1: Schematic of the grating-assisted wavelength channel add/drop filter for wavelengths both on and off resonance.

Integrated Optics Devices V, Giancarlo C. Righini, Seppo Honkanen, Editors,
Proceedings of SPIE Vol. 4277 (2001) © 2001 SPIE · 0277-786X/01/$15.00

2.2 Polarization Independent Operation

Polarization independent operation of the add/drop filter is critical. Surface relief gratings show higher loss and an intrinsic polarization dependence[6]. For these reasons, the Bragg gratings will be photowritten volume gratings. The silicate glass BGG31[7] will be used as a substrate for device fabrication. This glass was specially designed for Ag^+ ion-exchange, both to minimize Ag^+ reduction to metallic silver and to give a linear dependence of refractive index change on Ag^+ concentration. This glass has demonstrated excellent photosensitivity in the absence of Ge-dopants and without pretreatment of any kind[3]. Photobleaching using the 248 nm KrF excimer laser radiation changes the absorption spectrum near 350 nm and appears to add a new absorption band near 520 nm. No noticeable changes to the absorption spectrum occur above 650 nm. This is critical to the fabrication of low-loss gratings at 1550 nm.

Photowritten volume Bragg gratings exhibit polarization dependence if the waveguides are birefringent. These gratings were first demonstrated in ion-exchanged channel waveguides using surface waveguides[8]. Dips in transmission of almost 20 dB were characterized, with a TE-TM shift of 0.56 nm. The polarization dependence of the gratings was due to the birefringence of surface waveguides resulting from the asymmetry in the waveguide shape and stress. It was later shown that field assisted burial is an effective and flexible method for removal of the birefingence[9]. Identical gratings were written in waveguides of varying mask opening width and burial depth. Some results are shown below in Figure 2. A shallow burial depth of 2.8 microns already reduced the TE-TM shift to 0.1 nm. Burials 5.6, 8.4 and 13.8 microns deep all revealed a negligible shift of about 0.01 nm. Additionally, the polarization dependence was shown to be independent of the mask opening widths from 1-2.5 microns. So for our add/drop filter we fabricate buried ion-exchanged waveguides, since they have demonstrated the flexibility to produce non-birefringent waveguides for the device.

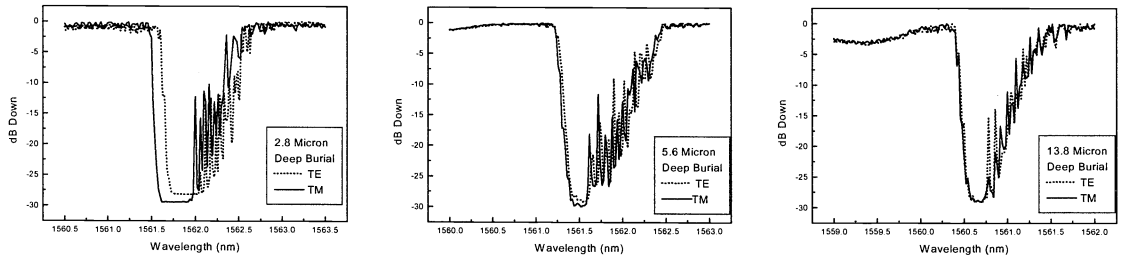

(a) (b) (c)

Figure 2. Polarization dependence of Bragg grating for burial depths of (a) 2.8, (b) 5.6 and (c) 13.8 microns.

3. Fabrication

3.1 Waveguide Fabrication

For fabrication of the add/drop filter, surface waveguides were formed in borosilicate glass by silver ion-exchange. A detailed discussion of the process, shown in Figure 3, can be found in lierature[1]. A 2 mm thick sample of BGG31 was coated with a 100 nm thick Ti mask layer. This mask was patterned with the add/drop design using standard photlithographic processes. The mask was oxidized for 1 hour in a sodium nitrate salt melt at 380 degrees C. The sample was then placed into a 50% silver nitrate salt melt at 300 degrees C for 15 minutes. The Ti mask was removed and the waveguides were buried for 5 minutes with a voltage of 310 V. Finally, the sample was cut and the end facets were polished. Modeling predicts that for the chosen ion-exchange times, waveguides with 2 - 4 micron mask openings will be single mode and waveguides with 5 - 7 micron mask openings will be two-mode. The device was designed to have input/output single-mode waveguides widths of 2.5 and 3.5 microns, and a two-mode section width of 6 microns.

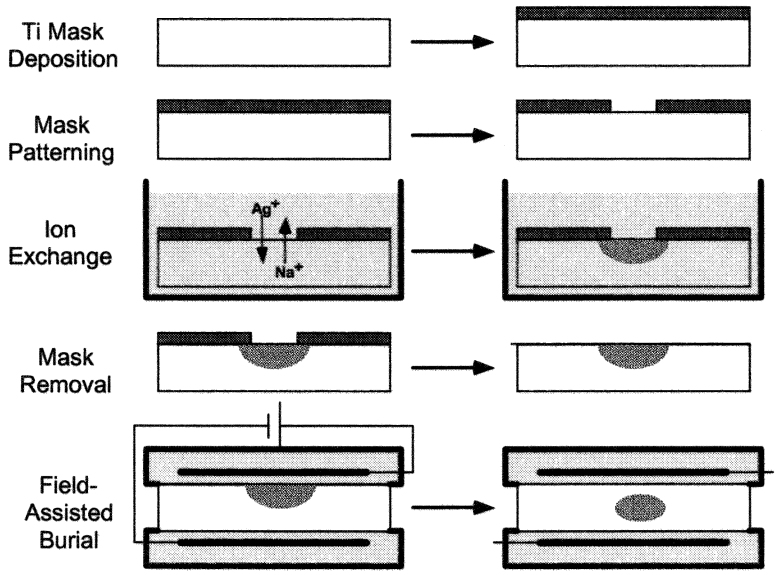

Figure 3. Fabrication of buried Ag ion-exchanged waveguides.

3.2 Grating Fabrication

Using a phase mask with a periodicity of 1070 nm, Bragg gratings were photowritten over the two-mode section of the devices. The exposure was masked using an aperture in the beam path. An area 8mm long by 2 mm wide was exposed for 12 minutes with 85 mJ per pulse and a pulse repetition rate of 50 Hz. The optimal grating angle for odd-even mode reflection was modeled to be around 3 degrees. The mask was designed such that a single exposure would expose identical devices at 1, 2, 3, and 4 degrees. However, difficulty in alignment leads to a margin of error of +/- 0.5 degrees.

4. Fabricated Device Performance

4.1 Asymmetric Y-Branch Performance

First, the operation of the asymmetric y-branch was characterized. Figure 4 shows mode pictures from a fabricated asymmetric y-branch. The input asymmetric y-branch works properly; the mode from the wider input guide gets coupled to the even mode of the two-mode guide and the mode from the narrower guide gets coupled to the odd mode of the two-mode guide. However, it is clear that the narrow input does not excite the odd mode perfectly. This is most likely due to imperfections in the photolithography, causing coupling between the two modes. This leads to some coupling to the wide waveguide output. This coupling was measured to be less than 6%: acceptable for this demonstration but too much for system level operation of a device.

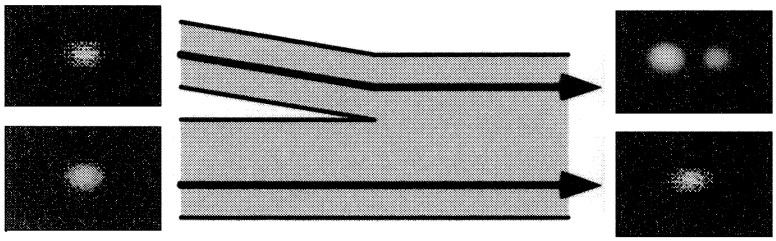

Figure 4. Mode pictures showing operation of input asymmetric y-branch.

4.2 Add/Drop Performance

A tunable laser was used to characterize both the transmission and reflection (out of the "drop" port) of the device. A polarization controller allowed characterization of both the TE and TM performance of the device. A polarizer was used at the output to ensure separation of the polarizations in transmission. It was also used to align the input polarization such that the orthogonal polarization was down by at least 20 dB for the reflection measurements where we were unable to use a polarizer. These measurements were done for both inputs to the device.

The performance of the device at the best grating angle is shown below in Figure 5. The device shows two sharp dips in transmission, although the second dip is very small for the narrow input at the best angle. Dips of over 20 dB demonstrate excellent reflection. The sharp dips at the shorter wavelength for the wide input and at the longer wavelength for the narrow input are at the same wavelength. The grating equation and the operation of the device tell us that these dips are the even-odd and odd-even mode reflections that are wanted for add/drop filtering. The other sharp dips are unwanted even-even and odd-odd mode reflection. The broad dip at short wavelengths for the wide input is most likely coupling to substrate modes.

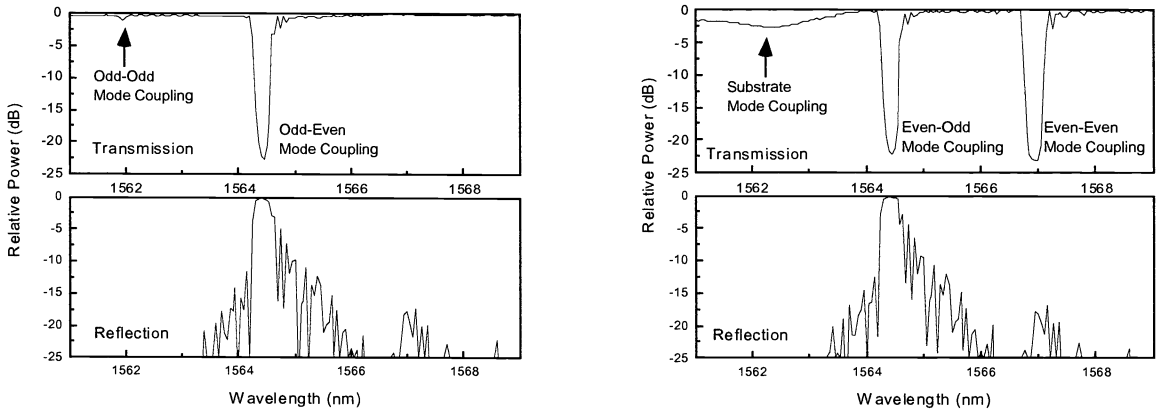

Figure 5. Transmission and reflection for both the (a) narrow and (b) wide input.

The conclusions are confirmed by looking at the reflection with the wide input, shown in Figure 5(b). The peak corresponding to the sharp dip at the shorter wavelength peak is much larger. It is much more effectively "dropped" out of the other port. The longer wavelength peak, even-even mode coupling, is almost non-existent as it is instead reflected back out the input port. It is possible to use the device effectively as an add/drop filter. Since the only critical function of the add and the drop ports is reflection out the other port, to the network it is insensitive to these unwanted dips. Using the wide input for adding/dropping, we are able to achieve the add/drop performance shown in Figure 6. Extinction ratios of over 20 dB and 3 dB bandwidths of 0.4 nm (100GHz) characterize the performance.

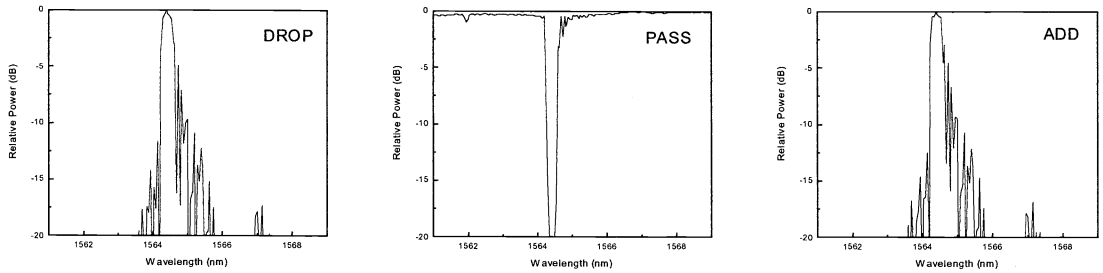

Figure 6. Add/drop performance of the filter.

4.3 Grating Angle

The possibility of having negligible odd-odd mode reflection while having significant even-even mode and even-odd mode reflection for a given grating angle is easily understandable. The cross coupling coefficient[10] is proportional to:

$$\kappa \propto \iint E_1 E_2 Exp[i2\pi x \tan\theta / \Lambda].$$

The larger size of the odd mode will make it more sensitive to the phase offset of the grating from the angle. The measured transmission dip of the even-even, odd-odd, and odd-even mode reflection is shown in Figure 7 for grating angles of 1-4 degrees. Also shown is the relative magnitude of the cross coupling coefficient predicted for the measured mode profiles. Although many more parameters are needed to accurately go from the cross coupling coefficient to the reflection dip, it is clear to see that the measured dips follows the general pattern predicted by the theory for the measured modes. It is interesting to note that the maximum cross coupling coefficient for odd-even mode coupling occurs at approximately the angle where there is a π phase difference in the grating contribution between the two lateral peaks of the odd mode.

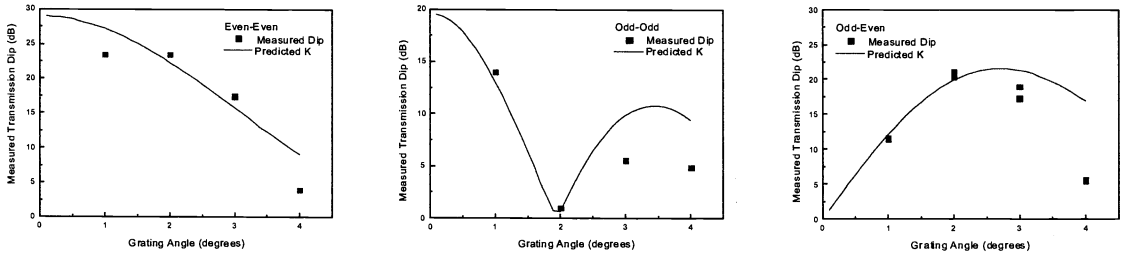

Figure 7. Dependence of predicted cross coupling coefficient and measured transmission dip on grating angle.

4.4 Polarization Dependence

The data presented so far is all for TM polarization. A polarization dependence of about 0.25 nm is seen looking in transmission at the odd-even mode dip of the narrow input, as shown in Figure 8. With DWDM channel spacings of as little as 50 GHz, this is obviously unacceptable. However, it is a significant reduction from the 0.8 nm shift that has been characterized for surface ion-exchanged waveguide gratings[8]. This, combined with previous results[9], shows simply that the burial of the device was not sufficient enough for polarization independent operation. A deeper burial in the final step of the ion-exchanged waveguide process should allow us to reduce this shift to negligible amounts while not affecting the performance of the rest of the device.

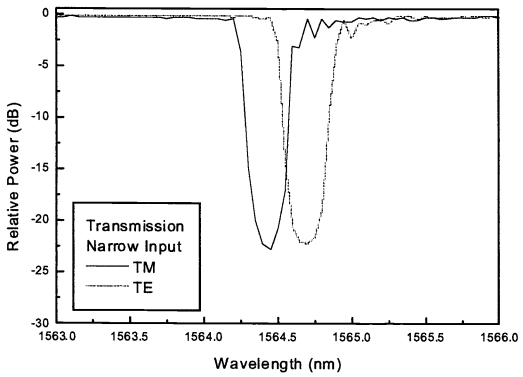

Figure 8. Polarization dependence of the add/drop filter.

5. Conclusions

In summary, we have demonstrated an add/drop filter using ion-exchange waveguide technology and photowritten Bragg gratings. The device exhibits 20 dB extinction ratios and 3 dB bandwidths of 0.4 nm (100 GHz), and a polarization dependence of about 0.25 nm. Further improvement to the performance can be achieved by grating optimization, a deeper burial step, and optimization of the modes sensitivity to angular misalignment.

Acknowledgements

This work was done as BMDO Phase I contract. The authors would like to acknowledge IOT for their partial support of this work.

References

1. S. I. Najafi, editor, *Introduction to Glass Integrated Optics*, Artech House, Norwood, MA, 1992.
2. P. Äyräs, G. Nunzi Conti, S. Honkanen, and N. Peyghambarian, "Birefringence control for ion-exchanged channel glass waveguides," *Appl. Opt.,* **37**, pp. 8400-8405, 1998.
3. D. Provenzano, W.K. Marshall, A. Yariv, D.F. Geraghty, S. Honkanen, and N. Peyghambarian, "Gratings formation in BGG31 glass by UV exposure," *Electron. Lett.*, **35**, pp. 1332-1334, 1999.
4. A.S. Kewitsch, G.A. Rakuljic, P.A. Willems, and A. Yariv, "All-fiber zero-insertion-loss add-drop filter for wavelength-division multiplexing," *Opt. Lett.*, **23**, pp. 106-108, 1998.
5. C.K. Madsen, T.A. Strasser, M.A. Milbrodt, C.H. Henry, A.J. Bruce, and J. Demarco, "Planar waveguide add/drop filter employing a mode-converting grating in an adiabatic coupler," *Integrated Photonics Research Tech. Dig.*, Victoria, BC, Canada, March 30 – April 1 1998, pp. 102-104.
6. M.J. Li, and S.I. Najafi, "Polarization dependence of grating-assisted waveguide Bragg reflectors," *Appl. Optics*, **32(24)**, pp.4517-21, 1993.
7. N. Fabricius, H. Oeste, H-J. Guttmann, H. Quast, and L. Ross, "BGG 31: A new glass for multimode waveguide fabrication," EFOC/LAN 88, Amsterdam, 1988.
8. D.F. Geraghty, D. Provenzano, W.K. Marshall, S. Honkanen, A. Yariv, and N. Peyghambarian, "Gratings photowritten in ion-exchanged glass channel waveguides," *Electron. Lett.*, **35**, pp. 585-587, 1999.
9. D. F. Geraghty, D. Provenzano, M. Morrell, J. Ingenhoff, S. Honkanen, A. Yariv, and N. Peyghambarian, "Polarization Independent Bragg Gratings in Ion-Exchanged Glass Channel Waveguides," *Electron. Lett.*, 36(6), pp. 531-532, 2000.
10. T. Erdogan, "Fiber Grating Spectra," *J. Lightwave Tech.*, **15**, pp. 1277-1294, 1997.